Preparation of Polypropylene–Clay Nanocomposites by the Co-Intercalation of Modified Polypropylene and Short-Chain Amide Molecules

U. N. Ratnayake,[1] B. Haworth,[2] D. J. Hourston[2]

[1]*Rubber Research Institute, Telawala Road, Ratmalana, Sri Lanka*
[2]*Institute of Polymer Technology and Materials Engineering, Loughborough University, Loughborough LE11 3TU, United Kingdom*

Received 24 January 2008; accepted 7 July 2008
DOI 10.1002/app.29371
Published online 29 December 2008 in Wiley InterScience (www.interscience.wiley.com).

ABSTRACT: The effect of short-chain amide (AM) molecules on the intercalation of montmorillonite clay has been investigated by the melt blending of polypropylene (PP) with clay in the presence of AM molecules such as 13-*cis*-docosenamide (erucamide). Polypropylene–clay nanocomposites (PPCNs) were prepared by the co-intercalation of maleic anhydride grafted polypropylene (PP–MA) and an AM compound. The resulting nanocomposite structures were characterized with X-ray diffraction (XRD) and transmission electron microscopy, whereas the thermal characterization of the PPCNs was conducted by thermogravimetric analysis. XRD results showed that the AM molecules intercalated into clay galleries and increased the interlayer spacing, a result confirmed by surface energy (contact angle) and melt flow index measurements. This additive allowed the formation of an intercalated nanocomposite structure, but an exfoliated PPCN structure was also formed with the use of AM with a PP–MA-based compatibilizer. A new preparation method for PPCNs was, therefore, developed by the co-intercalation of AM and PP–MA; this resulted in a significantly improved degree of intercalation and dispersion. The enhanced thermal stability of PPCN, relative to pure PP, further demonstrated the improved clay dispersion in the nanocomposite structures prepared by this method. A possible mechanism for the co-intercalation of AM and PP–MA into the clay galleries is proposed, based on hydrogen bonding between these additives and the silicate layers. Consideration is also given to possible chemical reactions and physical interactions in this rather complex system. J Appl Polym Sci 112: 320–334, 2009

Key words: additives; clay; compatibility; nanocomposites; poly(propylene) (PP)

INTRODUCTION

Polymer–inorganic nanocomposites are two-phase materials in which inorganic particles are dispersed at the nanometer range in the polymer matrix. Polymer nanocomposites based on montmorillonite (MMT) clay, which belongs to the general family of 2 : 1 layered silicates, have received increased attention[1–4] because they frequently show enhanced properties relative to the unfilled polymer and equivalent conventional composites at a lower concentration of clay. Generally, hydrophilic MMT is not compatible with most polymers, and, hence, it needs to be organically treated to make it more organophilic. A common method of organic treatment is the ion exchange of the cations within the clay with organic ammonium cations.[5,6] The Toyota Research Group first investigated polyamide 6/clay nanocomposites and found that the mechanical and thermal properties improved in comparison to both conventional microscale composites and the unmodified polymer at very low loading levels of clay.[7,8] Since then, a number of other polymer–clay nanocomposites, such as those based on polystyrene,[9] acrylic polymers,[10] epoxy resins,[11,12] and polypropylene (PP),[13–15] have been reported in the scientific literature.

PP is one of the most widely used thermoplastic materials for numerous applications, such as automotive and packaging applications, because of its versatility, overall balanced properties, ease of processing, and attractive property–cost ratios. However, it is difficult to disperse clay particles in a PP matrix, because the nonpolar PP is incompatible even with organically modified clays.[14,15] However, polypropylene–clay nanocomposites (PPCNs) have been prepared with functional oligomers that are compatible with both PP and organically modified clays.[1,13] The most commonly used compatibilizer for the preparation of PPCN is maleic anhydride grafted polypropylene (PP–MA).[13–15] Previous studies have examined the effect of PP–MA on the intercalation and exfoliation behavior of clay in a PP matrix, and

Correspondence to: B. Haworth (b.haworth@lboro.ac.uk).

TABLE I
Compositions of the PPCC Materials with Different Concentrations of the Short-Chain AM Compound

PPCC sample code	PP (wt %)	AM (wt %)	OMMT (wt %)
PP	100	—	—
PP-2	98	—	2
PP–AM0.3-2	97.7	0.3	2
PP–AM0.5-2	97.5	0.5	2
PP–AM0.7-2	97.3	0.7	2
PP–AM1-2	97	1	2
PP–AM1.5-2	96.5	1.5	2
PP–AM2-2	96	2	2

it has been revealed that, whereas the intercalation of clay is improved, fully exfoliated nanocomposite structures have not been achieved.[16–18] However, a high maleic anhydride concentration leads to phase separation, which therefore affects the achievable mechanical properties of the PPCN.[15,19] To improve the clay dispersability and to reduce the MA concentration, some studies have reported new ways of preparing PPCNs with secondary intercalant molecules.[20–22]

The objective of this study was to determine the effect of amide (AM) compounds on the intercalation and exfoliation of clay. On the basis of the diffusion behavior of the AM into the clay galleries, a new preparation method for PPCNs is proposed and was investigated by the co-intercalation of clay by PP–MA and AM. The diffusion of AM into the clay galleries and its interaction with clay was examined through shear flow properties [melt flow index (MFI)] and surface energy (contact angle) measurements. Possible reactions and interactions of these components in PPCNs and the thermal stability of PPCNs prepared by this co-intercalation method are also discussed.

EXPERIMENTAL

Materials

PP homopolymer grade HB671 supplied by Borealis (Beringen, Belgium) was used in this study; the MFI of this grade was 2 g/10 min when it was tested at 230°C with a 2.16-kg load. PP–MA (Polybond 3200, Crompton Corp., Middlebury, CT), containing 1 wt % maleic anhydride, was used as the functionalized polymer-based compatibilizer. MMT clay, modified with dimethyl dihydrogenated tallow quaternary ammonium chloride, was used to prepare the PPCNs and was supplied by Southern Clay Products (Gonzales, TX). Erucamide (13-*cis*-docosenamide) at 99.0% purity, supplied by Akzo Nobel Polymer Chemicals (Amersfoort, the Netherlands), was used as the short-chain AM component.

Melt mixing of AM with organically modified montmorillonite (OMMT)

OMMT was ground with AM powder in a specific ratio (i.e., 1 g of clay:0.25 g of AM) and heated in an oven at 100°C for about 30 min to allow the AM to diffuse into the clay galleries. The resultant organically modified montmorillonite treated with the amide (AM–OMMT) was analyzed by X-ray diffraction (XRD) to investigate the intercalation ability of this molecule into the clay galleries.

Preparation of the PPCNs

Polypropylene–clay composites (PPCCs) were prepared (without PP–MA) by the melt mixing of PP, OMMT, and different concentrations of AM to study the influence of AM on the intercalation and exfoliation behavior with a torque rheometer (Haake Rheomix 600, Waltham, MA) operating at 185°C (set temperature) and with a rotor speed of 100 rpm. The mixing time was 6 min for all composites. This condition was predetermined as the most appropriate mixing time. Table I presents the exact compositions of these composites.

PPCNs were prepared by the melt blending of PP with OMMT in the presence of both PP–MA and AM. The mixing conditions were the same as with the PPCCs, and the exact compositions of these composites are shown in Table II.

In all composites, the last digit of the sample code refers to the clay concentration. For example, PP–

TABLE II
Compositions of the PPCN Materials Prepared with PB Only and also with the AM Compound

PPCN sample code	PP (wt %)	PB (wt %)	AM (wt %)	OMMT (wt %)
PP–PB2-2	96	2	—	2
PP–PB6-2	92	6	—	2
PP–AM0.5–PB2-2 (PPCN2)	95.5	2	0.5	2
PP–AM1–PB4-4 (PPCN4)	91.0	4	1	4
PP–AM1.5–PB6-6 (PPCN6)	86.5	6	1.5	6
PP–AM0.5–PB4-2	93.5	4	0.5	2
PP–AM0.5–PB6-2	91.5	6	0.5	2

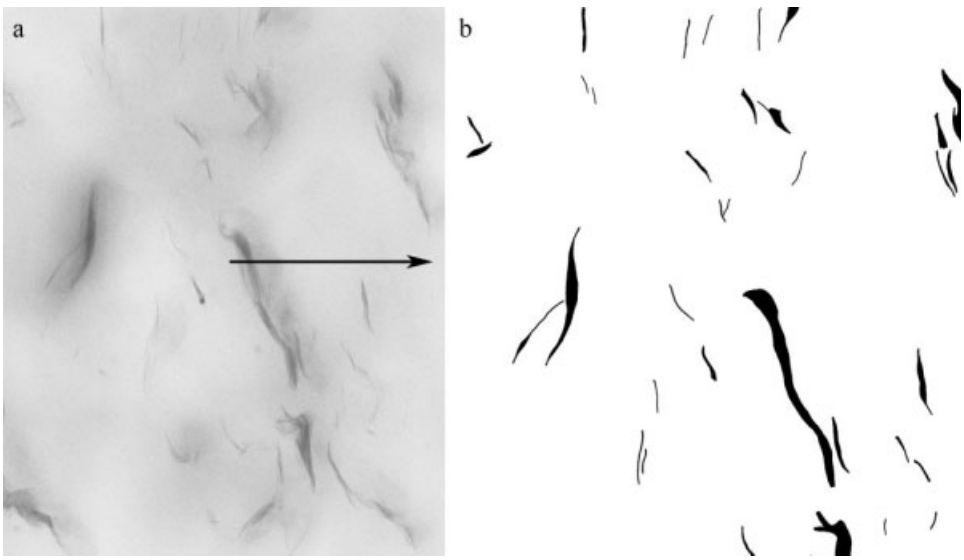

Figure 1 Conversion of a typical (a) TEM image into (b) a black-and-white image for subsequent image analysis.

PB6-2 and PP–AM0.5–PB2-2 refer to the PPCN prepared with 6 wt % PP–MA polymeric compatibilizer (PB) and 2 wt % clay and the PPCN prepared with 0.5 wt % AM, 2 wt % PB, and 2 wt % clay, respectively.

Characterization of the PPCN materials

XRD analysis was performed with a Bruker D8 diffractometer (Madison, WI) with Cu Kα radiation to determine the formation of nanocomposite structures and to determine the interlayer spacing of the clay in the PP matrix from the measured Bragg angles (2θ's). XRD patterns of thin compression-molded sheets of the PPCNs were obtained by scanning over a 2θ range from 1 to 10° at a rate of 0.01°/s. The conventional Bragg equation ($n\lambda = 2d \sin \theta$) was used to calculate the interlayer spacing of the clay in the composite materials. λ is the wavelength of the X-rays, d is the crystal lattice spacing, θ is the angle between the incident radiation and the scattering planes, and n is the order of reflection.

The degree of exfoliation of the clay and its dispersion into the PP matrix was also evaluated by transmission electron microscopy (TEM) with a Jeol model JEM 200FX electron microscope (Welwyn Garden City, UK) with an electron acceleration voltage of 200 kV. The degree of exfoliation was further studied for the PPCN materials prepared with PP–MA and AM with Image-Pro Plus analysis software (Bethesda, MD). TEM micrographs at 50,000× magnification were used for the image analysis. However, discrimination between gray polymeric regions and dark lines corresponding to clay platelets/stacks was not possible with this image analysis tool. Therefore, TEM images were converted into corresponding black-and-white images with enhanced contrast. The TEM images were first printed on A4 sheets; a piece of tracing paper was then placed on each printed image, and the dispersed clay platelets and/or stacks were traced over with a black permanent pen. Figure 1 shows the conversion of a TEM image into a resultant black-and-white image, which was electronically scanned and imported into the image analysis software. Clay particle (stack) thicknesses and their distribution in the PPCNs were obtained from the image analysis program. Clay stack thickness is inversely related to the degree of exfoliation.

Investigation of the interaction between the clay and the AM compound

MFI, in a pressure-imposed capillary shear flow experiment, was used to study the interaction of the AM with the clay in the melt state. MFI measurements of the PPCCs containing AM and the corresponding matrix (PP and AM only) were compared to examine any possible interaction between the AM and the clay in the melt state. The test temperature was set to 190°C, and a dead weight load of 2.16 kg was applied. Such short-chain AM molecules generally migrate to the surface when PP artifacts cool down because of incompatibility with the bulk PP.

The surface composition of the PPCCs prepared with the addition of AM was also examined qualitatively with contact angle measurements to characterize the surface of compression-molded thin films of these composite materials. The *contact angle*, the angle that a liquid (of known surface tension) makes while resting at thermodynamic equilibrium on a solid, is a measure of the wettability, or spreadability, of that solid surface, and this characteristic

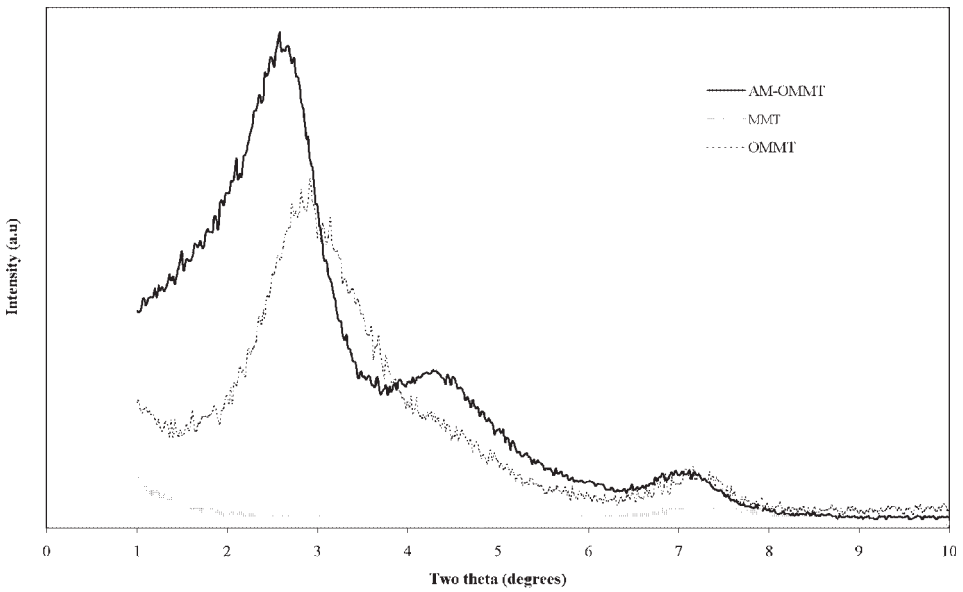

Figure 2 XRD patterns of the modified and unmodified clays.

varies greatly with the chemical nature of the solid surface in question. The advancing contact angle measurements of pure distilled water on the compression-molded thin films were measured with a Dataphysics OCA20 (an optical contact angle instrument) (Filderstadt, Germany) at room temperature (20°C). The molded films were analyzed for contact angles 10 days after the preparation of the samples as the surfaces were probably saturated with AM after that period of time. A small syringe was filled with pure distilled water, and the water was dispensed from the syringe at a rate of 2 μL/s to form drops on the film surface. For each sample, 12–15 contact angle measurements were taken from optical images of water drops on the surface, and for each image, the contact angle values were calculated on both edges with the software supplied with the instrument.

Fourier transform infrared (FTIR) spectroscopy was used to investigate the co-intercalation mechanism. A Mattson 3000 FTIR spectrometer (Hemel Hempstead, UK) was used for the analysis. The AM–OMMT was mixed with potassium bromide to make a pellet. AM powder (alone) was also used as a reference compound.

Thermal stability of the PPCNs

The thermal stabilities of the PPCN materials were investigated by thermogravimetric analysis (TGA), with a TA Instruments TGA 2950 instrument (New Castle, DE) at a heating rate of 15°C/min in an air environment. TGA and derivative thermogravimetry curves were obtained across a temperature range from 20 to 800°C.

RESULTS AND DISCUSSION

Intercalation of the AM additive

OMMT and AM–OMMT were characterized with XRD to examine the intercalation behavior of the AM into the clay galleries. Figure 2 shows the XRD spectra of the unmodified clay (MMT) and the modified clays (i.e., OMMT and AM–OMMT). When the unmodified clay (MMT) was organically modified (OMMT) with dimethyl dihydrogenated tallow ammonium ions, the characteristic diffraction peak (001) shifted from 7.22 to 2.96° because of an increase in the interlayer spacing from 12.2 to 30.2 Å. However, when OMMT was treated with the short-chain AM compound, the 001 diffraction peak shifted further to a lower 2θ (2.58°). As a result, the basal spacing increased from 30.2 to 34.2 Å. We suggest that when the OMMT powder was mixed with AM molecules and was heated to 100°C, the AM molecules intercalated into the clay galleries, and as a result, a higher interlayer spacing was achieved.

PPCCs (without compatibilizer) were prepared by the melt blending of PP and clay in the presence of the AM to examine the intercalation behavior of these molecules into the clay galleries during the melt-compounding process. The composites were again analyzed with the XRD technique. Figure 3 presents the comparison of the XRD patterns of a PPCC (PP–AM0.5-2) prepared by melt compounding of the PP with AM and OMMT and a PPCC (PP-2) prepared without the AM; the exact compositions of these composites are shown in Table I.

The characteristic diffraction peak (001) of OMMT is at 2.96° 2θ. The diffraction peak (001) for the PPCC (PP-2) prepared without the AM remained at

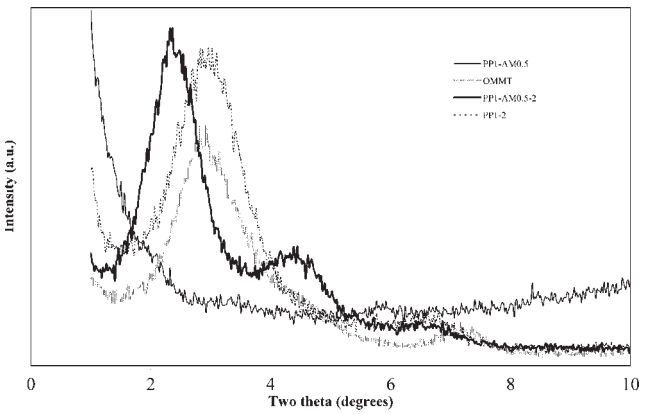

Figure 3 XRD patterns of the PPCCs prepared with 2% AM and also without the short-chain AM.

the same 2θ position as for the OMMT, which indicated no change in the interlayer spacing because the nonpolar PP did not intercalate into the clay galleries. In contrast, the XRD peak (001) of the PPCC (PP–AM0.5-2) prepared with 0.5 wt % AM shifted toward a lower 2θ, from 2.96 to 2.36°. This could be explained by the polar AM molecules intercalating into the OMMT galleries, and as a result, some PP chain segments were also more likely to diffuse into these clay galleries. The interlayer spacing of OMMT increased from 30.2 to 37.4 Å.

The driving force for the diffusion of AM into the clay galleries was likely to have been the attraction of the polar ($CONH_2$) group in the AM molecules to the polar sites of the silicate layers. These short-chain AM molecules were likely to have been bonded to the silicate layers by hydrogen bonding. However, although the diffraction peaks of both AM–OMMT and PP–AM0.5-2 were expected to be at the same 2θ (because both compounds had the same clay-to-AM ratio of 4 : 1), the diffraction peak of PP–AM0.5-2 was at a slightly lower angle (Fig. 3) of 2.36° than that of AM–OMMT (Fig. 2), which was at 2.58°. This was most probably because of the effective mixing involved in the Haake compounder when the PP–AM0.5-2 sample was prepared in comparison to the manual grinding of OMMT with AM. However, the 001 diffraction peak for the AM–OMMT became broader toward lower 2θ's (Fig. 2), which indicated the presence of clay stacks with a higher interlayer spacing.

Further investigations were undertaken to examine the effect of the AM concentration on the intercalation of the clay and to determine the AM concentration needed to achieve the maximum interlayer spacing. Figure 4 shows the XRD peaks of the PPCCs prepared with different concentrations of AM and 2 wt % clay (without PB) and demonstrates that all of the diffraction peaks (001) shifted to lower 2θ's when AM was incorporated into the PPCCs. The interlayer spacing of the clay increased with increasing AM concentration. Table II presents the 2θ positions and basal spacings. When 0.3 and 0.5 wt % AM were added to the PPCCs, the interlayer spacing of the clay was increased to 33.5 and 37.5 Å, respectively. However, increases in AM to 0.7 and 1 wt % were not effective (as shown in Table III) in terms of modifying the interlayer spacing further, probably because of the migration of the additional AM molecules to the surfaces, which occurred in pure PP.

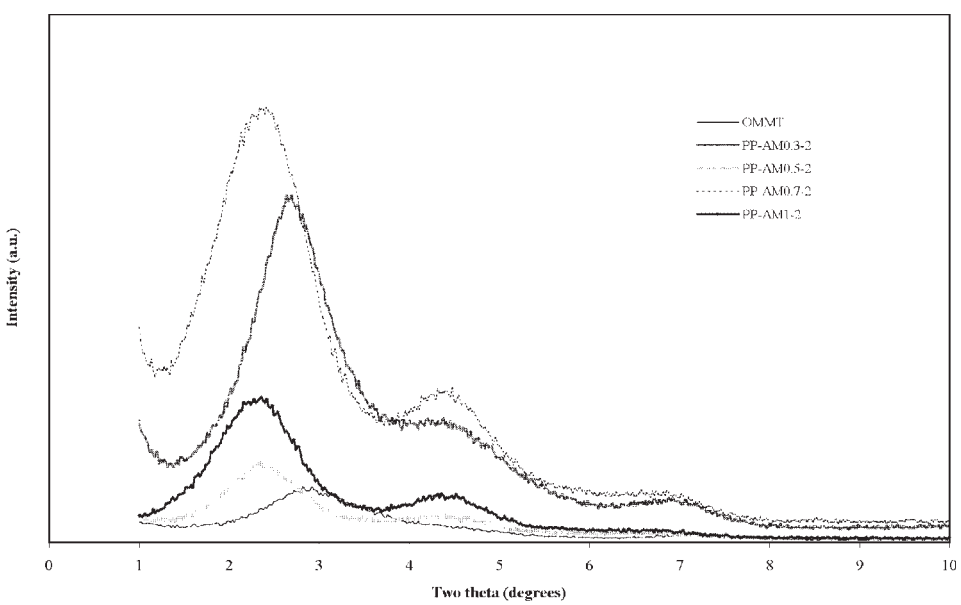

Figure 4 XRD patterns of the PPCCs prepared with different concentrations of short-chain AM between 0.3 and 1.0% (for 2% clay in PP).

TABLE III
Interlayer Distances of Clay in the PPCCs Prepared with Different AM Concentrations (from the XRD Data Shown in Fig. 4)

PPCN code	2θ (°)	Interlayer spacing (Å)
OMMT	2.92	30.2
PP–AM0.3-2	2.64	33.5
PP–AM0.5-2	2.36	37.5
PP–AM0.7-2	2.42	36.5
PP–AM1-2	2.36	37.4

We now consider the contact angle measurements of these composites to confirm the migration of additional AM onto the composite surfaces. The highest interlayer spacing was achieved by the addition of 0.5 wt % AM. This type of AM is generally incorporated into some PP formulations to reduce the surface friction[23] because it migrates onto the surface after processing due to its incompatibility with PP. To confirm the intercalation of AM and its interaction with clay, PPCC samples were prepared with different AM concentrations, and their corresponding blends (PP and AM only) were analyzed with contact angle and MFI techniques.

Figure 5 shows the MFI values of the PP–AM-2 composites prepared with increasing concentrations of AM (the exact compositions are shown in Table I) and the corresponding PP–AM blends. The MFI values of the PP–AM blends increased significantly with increasing AM concentration, in comparison to those of pure PP, and then started to level off when the AM concentration increased to more than 1 wt %. This was attributed to the AM, which acted as a flow-promoting species by increasing interchain motion in PP and by creating wall slip at the flow boundary under the constant applied shear stress (2.16-kg load) at 190°C. As a result, the melt viscosity of the PP–AM blends decreased markedly, which resulted in higher MFI values in the PP–AM blends.

However, with the addition of clay into the PP–AM blends, the MFI values were reduced dramatically compared to those of their corresponding PP–AM blends. When 2 wt % clay was added to the unmodified PP (Fig. 5), the MFI for the PP-2 composite decreased from 1.45 to 0.92 g/10 min. (i.e., a reduction of 37%) because of the increase in melt viscosity with the addition of clay. However, when the same clay weight percentage was added to the PP–AM blends (for AM concentrations up to 0.7 wt %), the MFI values for PP–AM-2 did not change significantly and remained similar to the MFI value of the control PP–clay-2 composite prepared without AM.

This implies that the AM molecules were not always present as free molecules in the PP–AM-2 composite melts to provide the flow modification effects on the PP compound, as discussed previously. This result supports the suggestion that most of the AM molecules diffused into the clay galleries, especially at low AM concentrations, when PP was under stress in its melt state. However, when the AM concentration was increased to more than 0.7 wt %, the MFI values increased because some of the AM molecules remained in the PP phase, which decreased the melt viscosity of these PP–AM-2 composites and resulted in comparatively higher MFI values. The XRD and MFI results suggest that the optimum AM concentration was around 0.5% when used with 2% clay in PP compounds.

Generally, when a short-chain AM is incorporated into pure PP, some molecules migrate to the surface, and a thin AM-rich layer is formed on cooling because of incompatibility with the PP matrix. As a result, the surface composition is changed. The contact angle is sensitive to the chemical nature of polymer surfaces. The water contact angles of the PPCC films prepared with the addition of different concentrations of the AM component were measured to characterize the accumulation of these molecules on the composite surface. Figure 6 shows the water contact angles for the PPCCs prepared with different concentrations of AM and their respective PP–AM blends.

The water contact angle of the pure PP film was 106°. However, when the AM was incorporated, the water contact angles of the PP–AM blends decreased significantly with increased AM concentration, in comparison to pure PP, and reached a steady value (at about 93°) with further increases in the additive concentration above 0.7 wt %. This implied an increased wettability and surface energy in the PP–AM blends due to the surface migration of AM. Constant values were obtained at higher concentrations of AM because the surface became saturated with AM molecules. There was no significant

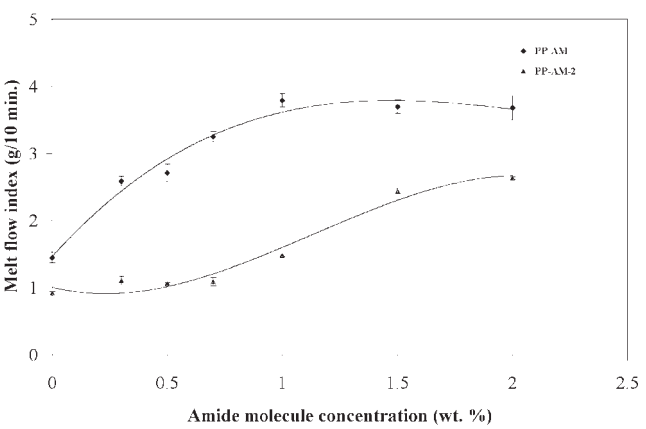

Figure 5 Effect of AM concentration on the MFI values of the PP–AM–clay composites (2% clay) and corresponding PP–AM blends.

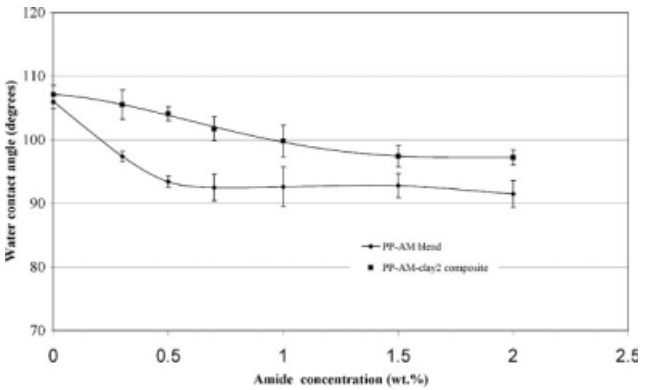

Figure 6 Water contact angles for the PP–AM blends and PPCCs (2% clay) prepared with different concentrations of AM.

difference in contact angles between PP and PP–clay-2 without AM (Fig. 6), which indicated that the addition of clay into pure PP did not change its surface properties. However, with the addition of clay (2 wt %) to the PP–AM blends, the water contact angles increased significantly compared to those of the respective PP–AM blends. When clay was added to the PP–AM0.3 blend, the water contact angle of the composite (PP–AM0.3–clay2) increased from 97.4 to 105.5°. Similarly, the water contact angle of the PP–AM0.5–clay2 composite increased by 10.7° compared to the corresponding blend (PP–AM0.5). This indicated that PP–AM–clay2 composites had comparatively lower wettability values than their corresponding blends because most of the AM molecules interacted with clay particles and did not migrate to the surface. At low concentrations especially (<0.7 wt % AM), most of the AM molecules intercalated and could not migrate to the surface. As a result, the water contact angles of PP–AM–clay2 became similar to the PP–clay2 composite. When AM was increased to more than 0.5 wt %, the water contact angles of the PPCNs were reduced toward the values of the PP–AM blends (without clay); because there was an excess of AM in the system, free AM molecules migrated to the composite surfaces, as occurred in the unfilled PP–AM blends.

Effect of the AM molecules on the clay dispersability

The XRD results, shear flow data, and contact angle measurements all confirmed the intercalation of AM into the clay galleries; so, the TEM micrographs of the PP–AM–clay composites were analyzed to evaluate the effect of AM on the clay dispersability in the PP matrix. Figure 7 shows the TEM micrograph of PP–AM–0.5-2, whereas Figure 8 shows the TEM micrograph of PP–clay (PP-2), which contained the same clay percentage as PP–AM0.5-2 but without

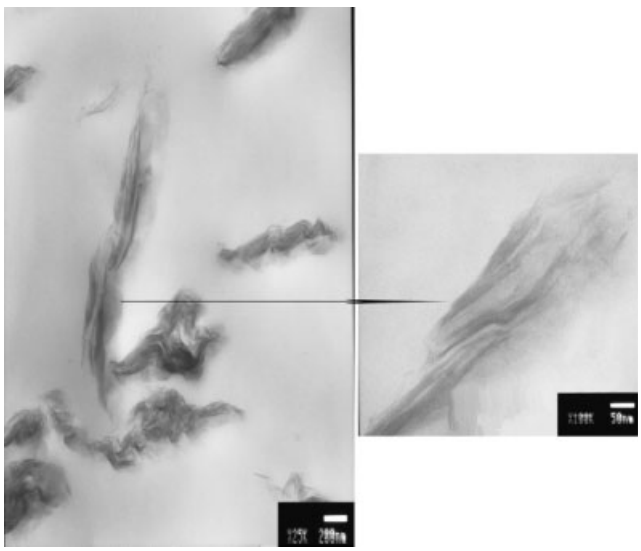

Figure 7 TEM micrographs of the PPCC (PP–AM-2, magnification = 25,000× on the left) prepared with the addition of AM. Scale bars indicate 200 nm (left) and 50 nm (right).

AM. The clay particles in both materials were not delaminated into smaller clay stacks, and they were not dispersed homogeneously throughout the PP matrix. PP–AM0.5-2 contained slightly bigger clay stacks than PP-2 because AM intercalated into the clay galleries and increased the interlayer spacing; this was in agreement with the XRD results shown earlier in Figure 3. However, the clay particles were not exfoliated, and as a result, the organized clay structure remained unchanged, which resulted in comparatively bigger clay particles for PP–AM0.5-2.

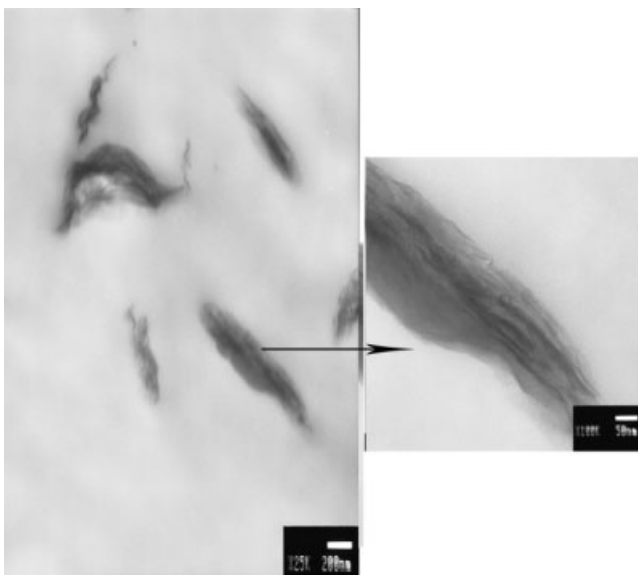

Figure 8 TEM micrographs of the PPCC (PP-2, magnification = 25,000 on the left) without AM. Scale bars indicate 200 nm (left) and 50 nm (right).

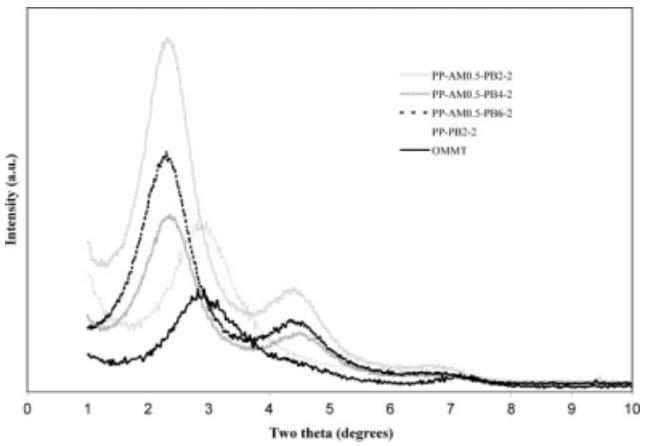

Figure 9 XRD patterns of PPCNs prepared with AM and different concentrations of PP–MA.

As shown by the TEM micrograph of PP–AM0.5-2 (Fig. 7) at higher magnification, clearly, the clay particles consisted of regions of alternating dark and light bands, which suggests that the AM compound was likely to promote the intercalation of PP chain segments into the clay galleries. However, the TEM micrograph of PP-2 (Fig. 8), at the same magnification, did not show a similar structure; no intercalation took place because of the absence of AM.

This confirmed that an intercalated clay structure was formed, as already suggested from the XRD results, when AM was incorporated into the PPCCs. Although the clay particles were intercalated, they were not exfoliated nor dispersed homogeneously throughout the PP matrix in the presence of AM only (i.e., during the compounding process) because the compatibility between the clay and the bulk PP was not improved significantly. Therefore, the addition of AM into the PPCCs created an intercalated and nonhomogeneously dispersed clay structure.

Co-intercalation of AM and PP–MA (PB)

The clay particles did not exfoliate toward the nanometer scale in the presence of AM alone, so PP was then melt-blended with clay in the presence of both AM and PP–MA to prepare PPCN structures with a Haake rheometer. The exact compositions of the PPCN materials were shown in Table II. Figure 9 presents the XRD spectra for the new PPCN materials (containing both AM and PP–MA) and conventional PPCNs prepared by the melt blending of PP with OMMT in the presence of PP–MA only. Table IV shows the (001) diffraction peak positions and interlayer spacing for each nanocomposite material. The diffraction peaks of all of the PPCNs prepared with both AM and PP–MA shifted to lower 2θ's compared to the conventional PPCN prepared with PB alone (i.e., PP–PB2-2). For example, the diffraction peak position of PP–AM0.5–PB2-2 shifted from 2.76° (i.e., the original peak position of PP–PB2-2) to 2.36° when 0.5 wt % AM was incorporated into the PP–PB2-2 material; as a result, the interlayer spacing increased from 31.3 Å (the interlayer spacing of PP–PB2-2) to 37.4 Å, which suggests that both AM and PP–MA co-intercalated into the clay galleries because each of these was compatible with OMMT.

The (001) diffraction peak did not shift to a lower 2θ when the PP–MA (PB) concentration was increased further (to 4 or 6%); it remained at 2.36° for all of the co-intercalated PPCN samples. The highest interlayer spacing was, therefore, achieved with 0.5 wt % AM and a relatively low concentration of PP–MA (2 wt %); further increases in the compatibilizer content were not effective in terms of increasing the interlayer spacing. However, the intensities of the diffraction peaks of the PPCNs prepared with higher concentrations of PP–MA (PP–AM0.5–PB4-2 and PP–AM0.5–PB6-2) were lower than those of the PPCN prepared with 2% PP–MA (PP–AM0.5–PB2-2). This might have been due to a comparatively higher degree of exfoliation achieved with higher concentration of PP–MA. However, the interpretation of peak intensity and its dependence on the degree of exfoliation is complex and subject to inaccuracy because the overall number of clay particles present in the sample can affect the peak intensity data.

Therefore, TEM analysis was arguably a more appropriate method for studying the clay dispersion in these PPCN materials, so TEM was performed on the conventional PPCN materials (prepared with PP–MA only) and also on PPCNs prepared by the co-intercalation of AM and PP–MA to evaluate the effect of both these additive systems on the clay dispersability in the PP matrix. Figure 10(a,b) shows the TEM micrographs of PP–PB2-2 and PP–AM0.5–PB2-2, respectively, showing the striking differences in the clay dispersion in the PP matrix between the conventional PPCN (PP–PB2-2) and the PPCN material (PP–AM0.5–PB2-2) prepared by the new co-intercalation method. As shown in Figure 10(a), most of the clay particles were not exfoliated into smaller stacks and were not dispersed uniformly

TABLE IV
Interlayer Spacing of the PPCN Materials Prepared with Different Concentrations of PB (from the XRD Data Shown in Fig. 9)

PPCN code	2θ (°)	Interlayer spacing (Å)
OMMT	2.92	30.3
PP–PB2-2	2.76	31.3
PP–AM0.5–PB2-2	2.36	37.4
PP–AM0.5–PB4-2	2.36	37.4
PP–AM0.5–PB6-2	2.36	37.4

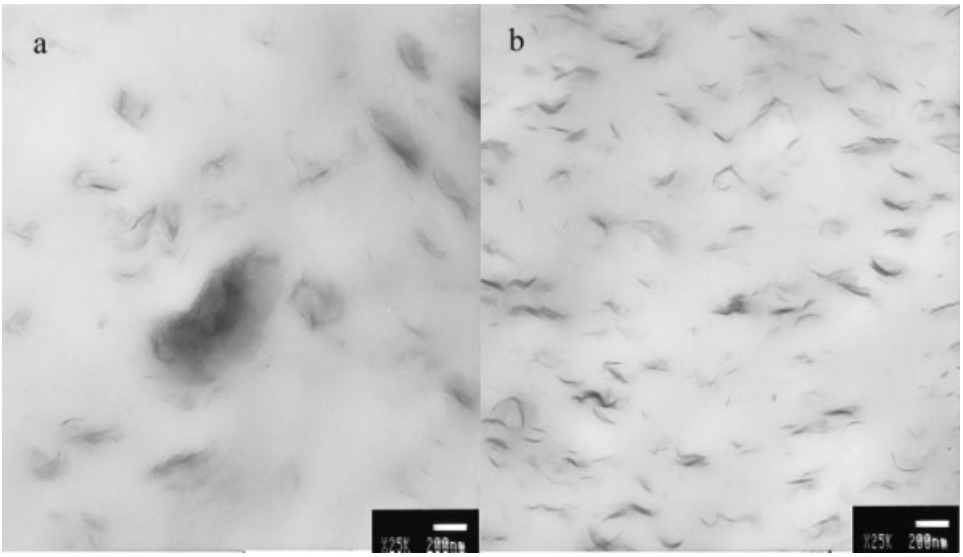

Figure 10 TEM micrographs showing different clay dispersabilities in a conventional PPCN and a co-intercalated PPCN, respectively: (a) PP–PB2-2 and (b) PP–AM0.5–PB2-2 (magnification = 25,000×, scale bar = 200 nm).

throughout the PP matrix. The large dark areas in Figure 10(a) were attributed to low exfoliation levels of clay particles when PPCN was prepared with a low concentration of PP–MA (i.e., a clay-to-PP–MA ratio of 1 : 1) because the compatibility between the clay and PP was not enhanced with a low concentration of PP–MA.[24] As a result, the deformational energy transferred from the PP matrix to the clay particles was not sufficient to create significant exfoliation during the compounding process. It has been reported that a high concentration of PP–MA (i.e., a clay-to-PP–MA ratio of 1 : 3) improves the clay dispersion because of its compatibility with PP.[24,25]

However, when the PPCN was prepared by the co-intercalation method [Fig. 10(b), PP–AM0.5–PB2-2] the clay particles were broken down into thinner stacks containing fewer individual clay layers and were dispersed more homogeneously throughout the PP matrix. Therefore, these TEM micrographs [Fig. 10(a,b)] confirmed that the incorporation of AM (along with PP–MA) into these PPCN structures significantly enhanced the degree of clay exfoliation. Improved clay dispersion was also achieved because both AM and PP–MA intercalated into the clay galleries, which resulted in a higher interlayer spacing, as shown in the XRD results (Fig. 9). Therefore, the

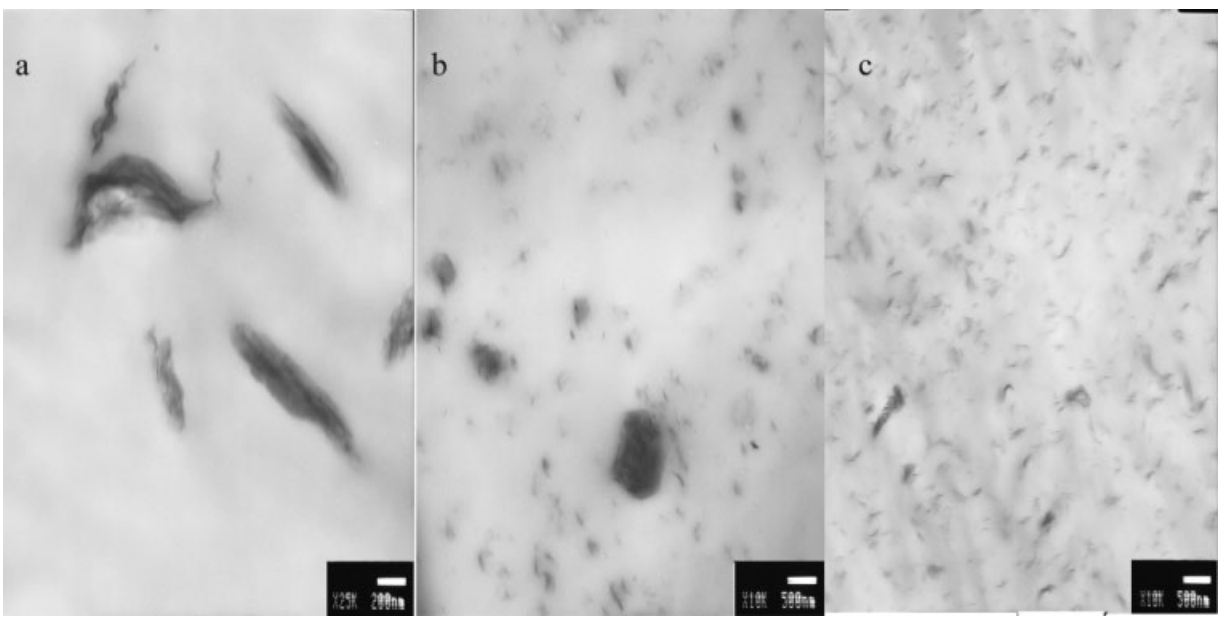

Figure 11 Clay dispersion as function of increasing PP–MA concentration in conventional PPCNs: (a) PP-2 (magnification = 25,000×), (b) PP–PB2-2, and (c) PP–PB6-2 (each at a magnification of 10,000×).

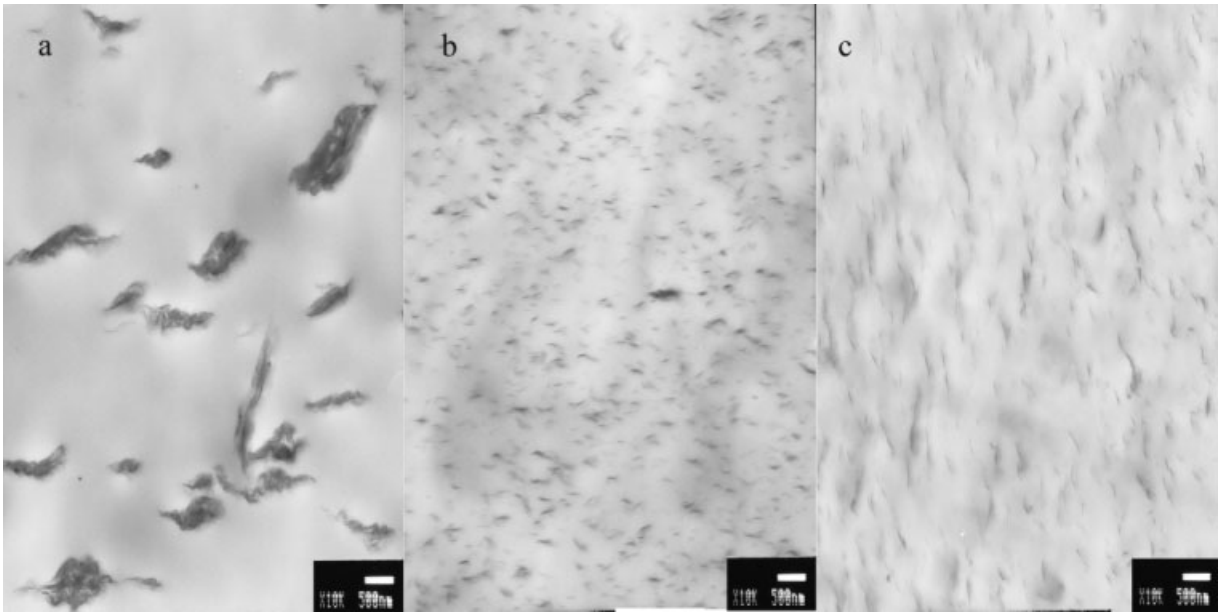

Figure 12 Clay dispersion as a function of increasing PP–MA concentration in PPCNs prepared by the co-intercalation method: (a) PP–AM0.5-2, (b) PP–AM0.5–PB2-2, and (c) PP–AM0.5–PB4-2 (magnification = 10,000×, scale bar = 500 nm).

attractive forces between the clay layers became weaker, so the clay particles were dispersed more homogeneously throughout the PP matrix during the compounding process, even with lower concentrations of PP–MA.

TEM images of PPCNs at lower magnification were prepared to compare the clay dispersion in the conventional PPCN (i.e., with only PP–MA as the PB) and in PPCNs prepared by the co-intercalation method (i.e., with both PP–MA and AM). Figure 11(a–c) shows how the clay dispersion was enhanced with an increase in the PP–MA concentration relative to the clay concentration in the PP nanocomposite. When a relatively low concentration of PP–MA (clay-to-PP–MA ratio = 1 : 1) was incorporated, the clay dispersion improved significantly [Fig. 11(b)] in comparison to the PP–clay microcomposite in which no compatibilizer was used [Fig. 11(a)]. However, a further increase in the PP–MA concentration [Fig. 11(c), clay to PP–MA ratio of 1 : 3] showed the greatest improvement in clay dispersion because a high PP–MA-to-clay concentration further improved the compatibility between the MMT clay and the PP matrix.

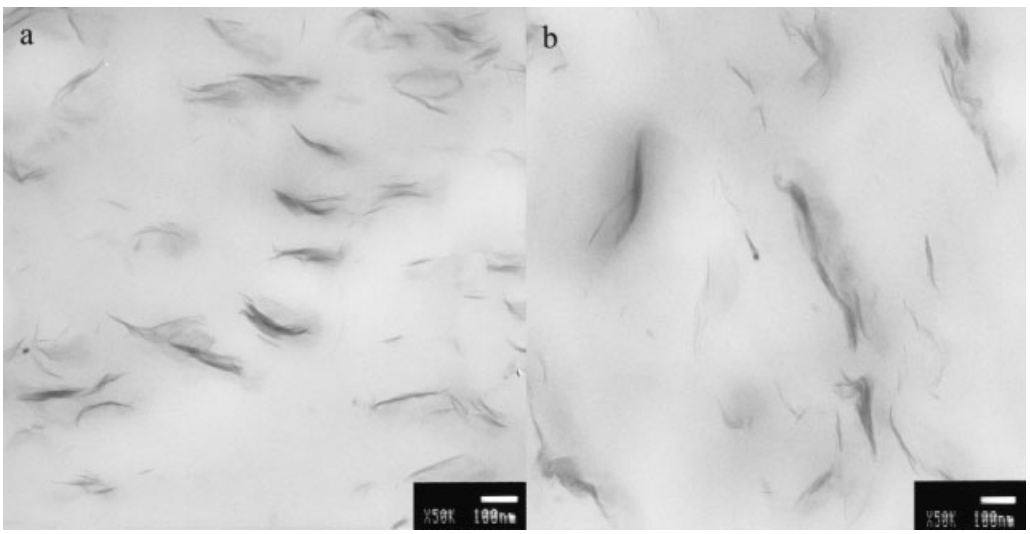

Figure 13 TEM micrographs at a higher magnification (50,000×, scale bar = 100 nm) of PPCNs prepared by the co-intercalation of PP–MA and AM: (a) PP–AM0.5–PB2-2 and (b) PP–AM0.5–PB4-2.

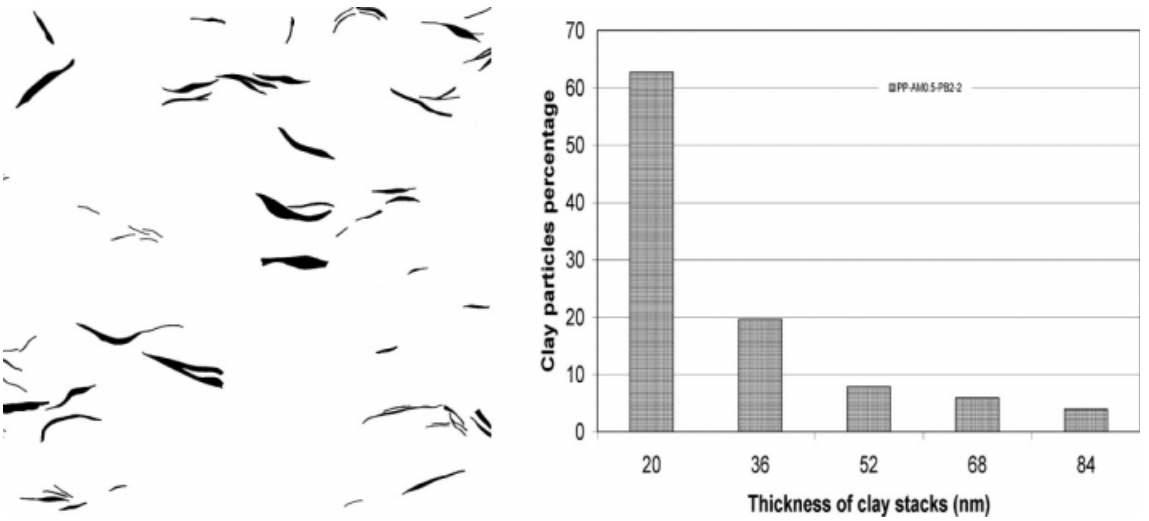

Figure 14 Image analysis of PP–AM0.5–PB2-2: (left) TEM image and (right) size distribution data for clay stack thickness.

In comparison to the conventional PPCN morphologies (Fig. 11), the PPCN structures [Figs. 12(b,c)] prepared by the new co-intercalation method showed improved dispersion of the clay. Figure 12(a) (PP–AM0.5-2) shows an intercalated but nonhomogeneously dispersed clay structure because of the absence of PP–MA. However, in contrast to the conventional method, PPCNs prepared with lower concentrations of PP–MA in combination with AM [clay-to-PP–MA ratios = 1 : 1 and 1 : 2 in Fig. 12(b,c)] showed a significant improvement in clay dispersion. There was no significant difference in clay dispersion between PP–AM0.5–PB2-2 and PP–AM0.5–PB4-2; optimum dispersion was achieved with around 2% PP–MA in combination with 0.5 wt % AM.

TEM of the PPCN structures: Image analysis

Examination of the nanocomposite structures (PP–AM0.5–PB2-2 and PP–AM0.5–PB4-2) at higher magnification [see Fig. 13(a,b)] further verified the XRD results (Fig. 9) in that they were mainly intercalated nanocomposite structures containing significantly smaller clay stacks (fewer clay layers per stack). However, the intercalated clay stacks were of different sizes, and, hence, the size distribution was determined with the image analysis software to quantify the degree of exfoliation achieved by the co-intercalation method.

The quantification of clay stack thickness (Figs. 14 and 15) clearly showed that the PPCN materials

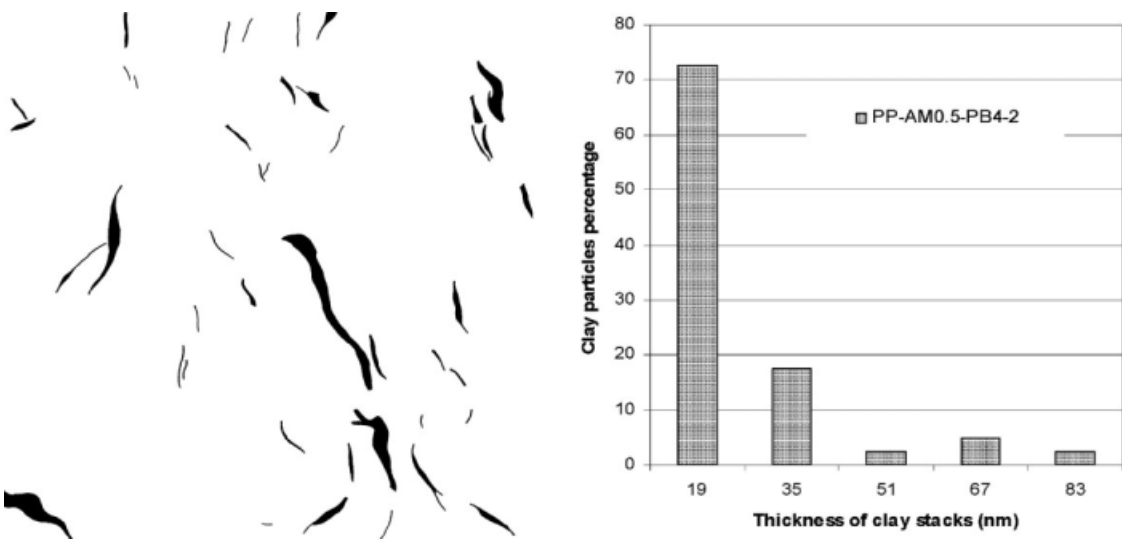

Figure 15 Image analysis of PP1–AM0.5–PB4-2: (left) TEM image and (right) size distribution data for clay stack thickness.

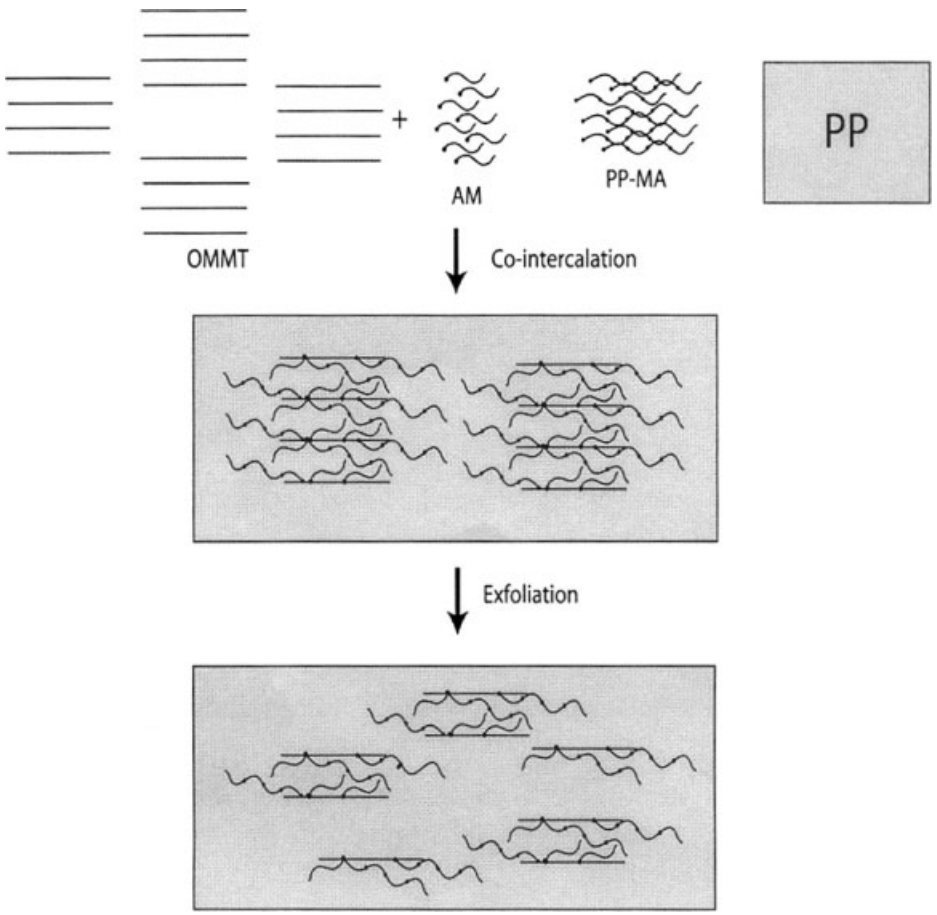

Figure 16 Schematic illustration of PPCN preparation by the co-intercalation of AM and PP–MA.

prepared with both PP–MA and AM contained very thin clay stacks. Both nanocomposite structures showed a similar distribution of clay stack thickness; about 60–70% of the clay particles were exfoliated to stacks less than 20 nm thick, and around 90% of the clay stacks were less than 52 nm thick. Although these observations were true for each PPCN material, there was a relatively small improvement in size distribution for the compound prepared with 4% PP–MA (Fig. 15). Overall, these results suggest that PPCN structures can be prepared with a high degree of exfoliation by the new co-intercalation method, although these PPCNs are essentially still intercalated structures. Figure 16 shows a schematic illustration to describe the co-intercalation of AM and PP–MA into the clay galleries.

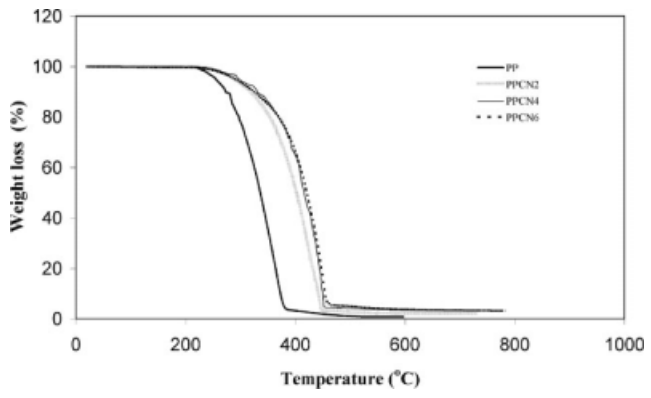

Figure 17 TGA curves of PP and PPCNs with different clay concentrations (0–6%).

Thermal stability of the PPCN materials

The thermal stabilities, for which nanocomposite morphology plays an important role, of the pure PP and PPCNs were analyzed with TGA in an air environment. Figure 17 shows the TGA curves for the pure PP and PPCNs with different clay concentrations, and Table V presents the temperature corresponding to 10% weight loss (T_{10}; which is

TABLE V
TGA Data for the PP and PPCNs with Different Clay Concentrations

Code	T_{10} (°C)	T_{50} (°C)	T_{max} (°C)
PP	273	336	368
PPCN2	318	402	424
PPCN4	330	416	448
PPCN6	324	421	450

considered as the onset of degradation), the temperature corresponding to 50% weight loss (T_{50}), and the temperature at which maximum rate of weight loss (T_{max}) values obtained from the TGA and derivative thermogravimetry curves. The incorporation of clay into PP significantly enhanced the thermooxidative stability, compared to unmodified PP. The thermal stability increased only marginally when the clay concentration was increased above 2 wt %. The onset of the thermal degradation of PP (T_{10}) was about 273°C in a static oxidative environment. However, the onset of thermal degradation for the PPCN containing 2 and 4 wt % clay (PP–AM0.5–PB2-2 and PP–AM1–PB4-4) increased by 45 and 57°C, respectively, compared to PP (see Table V).

Data for the values of T_{50} were parallel with the degradation onset temperatures and shifted markedly toward higher temperatures when the clay was introduced into PP. T_{50} values for PP–AM0.5–PB2-2 (PPCN2) and PP–AM1–PB4-4 (PPCN4) increased from 336°C (T_{50} for pure PP) to 402 and 416°C, respectively; the addition of 6% clay (PP–AM1–PB4-6) produced only a very marginal improvement in stability. Similar trends were obtained for T_{max} (from the maximum in the derivative data), which indicated reduced degradation rates and weight losses in all PPCN materials relative to the unmodified PP.

A similar enhancement in thermal stability by the introduction of an organically modified clay was reported for PPCN.[26–29] Zanetti et al.[30] studied the thermooxidative degradation of PPCNs with the TGA method and observed that the nanocomposites were more stable than the neat PP; the authors proposed a mechanism whereby oxygen attacked the PP chain by hydrogen abstraction at the methine carbons. Therefore, the enhanced thermal stability of the PPCNs, in an oxidative environment, was explained by the exfoliated and well-dispersed clay particles acting as an enhanced barrier to reduce the oxygen permeability rate into the nanocomposite structure and, at the same time, to reduce the diffusion of volatile degradation products from the composite matrix to the gaseous phase. This improved thermal stability of the PPCNs further confirmed the desirability of the nanocomposite morphology obtained by the co-intercalation of PP–MA and the short-chain AM compound.

Mechanism of co-intercalation

XRD and contact angle measurements showed that the short-chain AM diffused into the clay galleries and interacted with them; the FTIR spectra of the AM–OMMT were then analyzed to investigate the co-intercalation mechanism. Figure 18 shows the FTIR spectra of the AM–OMMT mixture and the

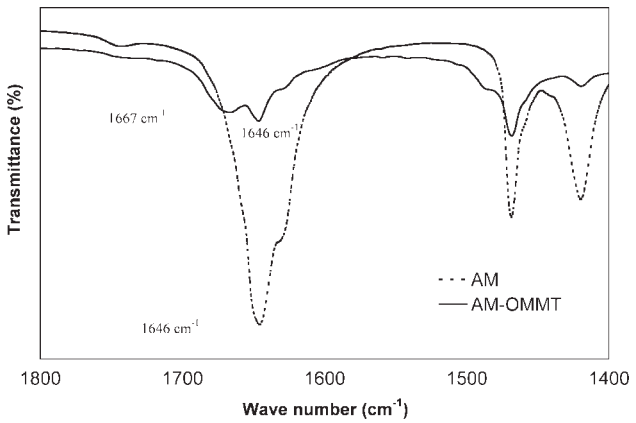

Figure 18 FTIR spectra of the carbonyl regions (C=O) for the AM and AM–OMMT samples

AM alone. The FTIR spectrum of AM–OMMT showed a doublet (1646 and 1667 cm^{-1}) for the peak corresponding to C=O stretching vibration compared to the single peak (1646 cm^{-1}) for pure AM. Although we expected that the C=O peak would shift toward a lower wave number because of hydrogen bonding between the C=O groups in AM and the O—H groups in the silicate layer surfaces, the C=O peak of OMMT–AM shifted to a higher wave number (1667 cm^{-1}). This was because AM exhibited intermolecular hydrogen bonding, and as a result, the C=O peak appeared at a lower wave number (1646 cm^{-1}). However, when the AM was intercalated into the clay (Fig. 18: AM–OMMT), the AM molecules were largely dispersed at the molecular level within the clay galleries, and as a result, the C=O peak appeared as a doublet with a higher wave-number peak. The peak at 1646 cm^{-1} in AM–OMMT may have arisen from free dispersed AM molecules that were not within the clay galleries.

These FTIR results, along with the XRD data (i.e., an increase in interlayer spacing due to intercalation of AM), present strong evidence for the formation of hydrogen bonding between the silicate layers and AM. We suggest this as the thermodynamic driving force for the intercalation of AM into the clay galleries. This interaction prevented the diffusion of these short-chain AM molecules toward the composite surface, as would be anticipated in an unfilled grade of PP. However, when PPCN was prepared by the co-intercalation method, not only AM but also PP–MA was added. The addition of PP–MA may have resulted in more complex chemical interactions between these three components (i.e., the silicate layers, AM, and the maleic anhydride functional groups in PP–MA) in the melt state during the compounding process.

It is clear that the systems reported here were complex in that they may have contained up to five components: the organically modified clay, which

had both the quaternary ammonium salt and Si—OH groups on the surfaces of the silicate layers; the AM, $H_3C—(CH_2)_7—CH=CH—(CH_2)_{11}—CO—NH_2$, which had a double bond; PP, which had a methine hydrogen in each repeat unit, which was extractable in free-radical reactions; and, finally, maleated PP, which had both the aforementioned extractable methine hydrogen and the potentially reactive maleic anhydride groups.

The clay (OMMT) and AM were treated at 100°C for 30 min in an air oven. The compounding with the polymer was done at 185°C for 6 min at 100 rpm. These were certainly not extreme conditions, but it was unclear how conducive they were to initiating chemical reactions that affected the final morphology. To elucidate what reactions were possible, it will be necessary to conduct experiments on simplified and, most likely, model systems to check if potential reactions do in fact occur under the conditions used in this study. This would be a very substantial program of work and is clearly outside the scope of this initial report on the clear benefits of using two compatibilizing agents.

Nevertheless, it is sensible to discuss here, in general terms, the chemistry that might have occurred during sample preparation. If only reactions between pairs of the five components present are considered, 10 such possibilities must be assessed. Before we consider these possibilities, the reactions with air (oxygen) during processing should be considered. In the case of the clay–AM melt-mixing process at 100°C, it is unlikely that the conditions were sufficiently forcing to cause any reactions involving oxygen and the methine hydrogen atoms in AM. As PP and PP–MA were protected, as in standard practice, with an antioxidant, and the processing temperature was 185°C, common for PP, no significant degree of reaction with oxygen would be expected.

We now present some brief comments on the other possible pairwise reactions or interactions. First, consider the cases involving the rather acidic —OH groups on the silicate layer surfaces. Any reaction with AM was thought unlikely, but polar interactions with the AM group were likely. The silicate hydroxyl groups may have also exhibited polar interactions with the organic modifier in the clay, but these were unlikely to be important because of the extensive steric hindrance around the quaternary nitrogen atoms. No reactions would have occurred with the PP, but the maleic anhydride moieties in the PP copolymer could have been ring-opened by the acidic hydroxyl groups. The AM component was not likely to react with the quaternary ammonium salt (the organic modifier in the clay) or with the PP. However, an imidization reaction was very likely with the maleic anhydride groups in the modified PP compatibilizer. This is discussed further in terms of the available literature. The organic modifier would not have reacted with the PP nor probably with the maleated PP, but there could have been physical interactions between these two components. Finally, no reaction would have occurred between the PP and the maleated PP.

In the literature, the most frequent explanation for the intercalation of PP–MA into clay is a polar interaction between the maleic anhydride group of the functionalized PP and the silicate layers.[15,24] Okada and coworkers[15,25] pointed out the possibility of reacting PP–MA with octadecylamine (used for the organic modification of clay) and the possible formation of imide groups. However, Szazdi et al.[31] carried out a comprehensive study of the interactions between the components in PPCNs. They showed[31] that PP–MA could react with the organic modifier used in the clay if it contained active hydrogen atoms (hexadecylamine was used in their study), and this led to the formation of AMs. The possibility of the formation of cyclic imides was also recognized, but their existence was not proven because the characteristic vibration peak of the imide group appeared in the same range as the other peaks in the spectrum.

In our system, when PP–MA was melt-mixed with AM, there was also the possibility of the formation of imide groups by the reaction of the active H atoms of AM and the highly reactive maleic anhydride group of PP–MA. Such imide groups could have also interacted with the silicate layers through hydrogen bonding. However, the existence of imide groups could not be detected from FTIR spectroscopy because: (a) there was a very low percentage of maleic anhydride in the PPCN material and (b) there were overlapping peaks relating to the imide bond (1723 and 1777 cm^{-1}) and other peaks. Therefore, in this new intercalation method, we suggest that intercalation can occur by either AM and PP–MA separately or as a reacted product (imide) or both together.

CONCLUSIONS

The intercalation of a short-chain aliphatic AM (erucamide) into MMT clay galleries was investigated. XRD results reveal that the AM effectively intercalated into the galleries during the melt-mixing process with PP, which resulted in higher interlayer spacings than for the original, organically modified clay. MFI and contact angle measurements verified the XRD results, that these AM molecules intercalated the clay particles. Contact angle data confirmed that, as a result of the intercalation process, the AM did not migrate onto the composite surfaces, especially at low concentrations. However, the clay particles did not exfoliate or disperse homogeneously

throughout the PP in the presence of the AM alone, which resulted in a nonhomogeneously dispersed, intercalated clay structure. The addition of both PP–MA and the aliphatic AM significantly enhanced the clay exfoliation and its dispersion in the PP matrix, in comparison with conventional PPCNs prepared with PP–MA only. The thermal stabilities of the PPCNs prepared by the co-intercalation method were improved by the addition of this organically modified clay; the improvement in thermal stability relative to that of the unmodified PP further confirmed the improved clay dispersion in the nanocomposite structure.

This study demonstrates a new method of preparing PPCNs by the co-intercalation of PP–MA and an aliphatic AM, which allows a reduction in the maleic anhydride content in the nanocomposite structures. Such a system, containing potentially reactive components processed at a high temperature, is very difficult to understand in full detail. Some discussions of potential reactions have been included, but more work is needed on, initially at least, model compounds to confirm which, if any, of these reactions actually occurs.

References

1. Kawasumi, M.; Hasegawa, N.; Kato, M.; Usuki A.; Okada, A. Macromolecules 1997, 30, 6333.
2. Hasegawa, N.; Okamoto, H.; Kato, M.; Usuki, A. J Appl Polym Sci 2000, 18, 1918.
3. Kurokawa, Y.; Yasudo, H.; Kashiwagi, M.; Oyo, A. J Mater Sci Lett 1993, 16, 1620.
4. Yano, K.; Usuki, A.; Yurauchi, T.; Kamigaito, O. J. J Polym Sci Part A: Polym Chem 1993, 31, 2493.
5. Theng, B. K. G. The Chemistry of Clay–Organic Reactions; Wiley: New York, 1974.
6. Alexandre, M.; Dubois, M. Mater Sci Eng 2000, 28, 1.
7. Usuki, A.; Kawasumi, M.; Kojima, Y.; Fukushima, Y.; Okada, A.; Karauchi, T.; Kamigaito, O. J Mate Res 1993, 8, 1179.
8. Kojima, Y.; Usuki, A.; Kawasumi, M.; Okada, A.; Fukushima, Y.; Karauchi, T.; Kamigaito, O. J Mater Res 1993, 8, 1185.
9. Vaia, R. A.; Isii, H.; Gianneils, E. P. Chem Mater 1993, 5, 664.
10. Biasci, L.; Aglietto, M.; Ruggeri, G.; Ciardelli, F. Polymer 1994, 35, 3296.
11. Wang, M. S.; Pinnavaia, T. J. Chem Mater 1994, 6, 468.
12. Messerssmith, P. B.; Giannelis, E. P. J Polym Sci Part A: Polym Chem 1995, 33, 1047.
13. Usuki, A.; Kato, N.; Okada, A.; Karauchi, T. J Appl Polym Sci 1997, 63, 137.
14. Hasegawa, N.; Kawasumi, M.; Kato, M.; Usuki, A.; Okada, A. J Appl Polym Sci 1998, 67, 87.
15. Kato, M.; Usuki, A.; Okada, A. J Appl Polym Sci 1997, 66, 1781.
16. Garicia-Lopez, D.; Picqazo, O.; Merino, J. C.; Paster, J. M. Eur Polym J 2003, 39, 945.
17. Wang, Y.; Chen, F.; Li, Y.; Wu, K. Soc Plast Eng Annu Tech Conf 2003, 61, 3670.
18. Perrin-Sarazin, F.; Ton-That, M. T.; Bureau, M. N.; Denault, J. Polymer 2005, 46, 11624.
19. Nara, K. A. Soc Plast Eng Annu Tech Conf Proc 2003, 61, 3717.
20. Liu, X.; Wu, Q. Polymer 2001, 42, 10013.
21. Zang, Y.; Lee, J.; Rhee, J. M.; Rhee, K. Y. Compos Sci Technol 2004, 64, 1383.
22. Zang, Y.; Lee, J.; Jang, H.; Nah, C. Compos B 2004, 35, 133.
23. Wypych, W. Handbook of Antiblocking, Release, and Slip Additives; Chemtec: Toronto, Canada, 2005.
24. Ray, S. S.; Okamoto, M. Prog Polym Sci 2003, 28, 1539.
25. Usuki, A.; Kato, M.; Okada, A.; Karauchi, T. J Appl Polym Sci 1997, 63, 137.
26. Tidjani, A.; Wald, O.; Pohl, M.; Hentschel, M.; Schartel, B. Polym Degrad Stab 2003, 82, 133.
27. Modesti, M.; Lorenzetti, A.; Bon, D.; Besco, S. Polym Degrad Stab 2006, 91, 672.
28. Tang, Y.; Hu, Y.; Song, L.; Zong, R.; Gui, Z.; Chen, Z. Polym Degrad Stab 2003, 82, 127.
29. Su, S.; Wilkie, C. A. Polym Degrad Stab 2003, 83, 347.
30. Zanetti, M.; Camino, G.; Reichert, P.; Mulhaupt, R. Macromol Rapid Commun 2002, 22, 176.
31. Szazdi, L.; Pukanszky, J. B.; Foldes, E.; Pukanszky, B. Polymer 2005, 46, 8001.